Effect of Nanostructured Ceramic Additives on the Mechanical Properties of Welded Joints

Rustam Saidov

Institute of Material Sciences of the Uzbekistan Academy of Sciences, Changikhisarak, Tashkent Region, Uzbekistan saidov_r@yahoo.com

Rustam Rakhimov

Institute of Material Sciences of the Uzbekistan Academy of Sciences, Changikhisarak, Tashkent Region, Uzbekistan rustam-shsul@yandex.com

Kamel Touileb

Department of Mechanical Engineering, College of Engineering in Al-Kharj, Prince Sattam bin Abdulaziz University, Al-Kharj, Saudi Arabia K.touileb@psau.edu.sa (corresponding author)

Joffin Ponnore

Department of Mechanical Engineering, College of Engineering in Al-Kharj, Prince Sattam bin Abdulaziz University, Al-Kharj, Saudi Arabia J.ponnore@psau.edu.sa

Received: 21 January 2025 | Revised: 12 February 2025 and 5 March 2025 | Accepted: 9 March 2025 | Licensed under a CC-BY 4.0 license | Copyright (c) by the authors | DOI: https://doi.org/10.48084/etasr.10306

ABSTRACT

The present work contributes to previous research regarding the influence of Photocatalyst Nanostructured Functional Ceramics (PNFC) additives on the welding and technological properties of welding electrodes of the MR-3 brand. It presents a comparative analysis of the properties of welded joints obtained during welding with the developed welding electrodes, with additives of PNFC brand ZB-2 (IMAN-8), and the ESAB E6013 welding electrodes. The focus was placed on the weld morphology, microstructure, and mechanical properties in Shielded Metal Arc Welding (SMAW). The results show that incorporating up to 2% PNFC ZB-2 in the electrode coating enhances melting efficiency, arc stability, weld formation, and the microstructural characteristics of the weld metal. Compared to ESAB E6013 electrodes, IMAN-8 electrodes exhibit better performance in arc penetration, weld metal structure, and mechanical properties of welded joints. From an economic perspective, IMAN-8 electrodes offer significant advantages over E6015 electrodes, reducing total welding time by up to 50%, lowering electrode and electricity consumption by approximately 50%, and cutting overall welding costs by nearly half. Also, the ability to weld thin sheets of carbon steel with IMAN-8 electrodes in one pass reduces the likelihood of defects requiring reworking the weld.

Keywords-SMAW; PNFC coating additive electrodes; mechanical properties

I. INTRODUCTION

This work focuses on SMAW, a versatile joining process for fabricating pressure vessels and boilers, which offers good quality welds and it is critical for manufacturing steel structures, particularly in the oil and gas sector [1, 2]. SMAW is a manual joining process characterized by its flexibility and transportability across various working conditions and environments [3]. However, its main drawback is the loss of

electrode material owing to the weld spatter. This affects productivity due to weld cleanup, and restoration [4].

Limited information is available about the use of nanostructured materials in the welding field, but research regarding their use has increased significantly in recent years. A major advantage of using nanomaterials is their ability to be tailored to specific requirements regarding size, shape, and properties [5]. A promising type of nanomaterial comes in the form of nano-powders, namely powders with a characteristic

nanoscale size, which leads to significant changes in their properties [6, 7]. Their use can significantly enhance existing technological processes and create new production methods. Authors in [8] demonstrated that nanosized refractory compounds, such as titanium carbide or nitride, improve the strength of laser-welded joints by refining their microstructure from needle-dendritic to quasi-equiaxed and finely dispersed, thereby enhancing mechanical properties, like strength and plasticity. Authors in [9] proposed adding nano-powder to the liquid glass during the production of electrodes to improve the mechanical properties of the weld metal. Authors in [5] later proposed modifying SMAW electrode production by introducing Ti, Zr, and Cs nano-powders into the electrode components via liquid glass, which enhances arc stability and weld strength. The RCrO₃ ceramic materials, where R represents a rare earth oxide, such as yttrium oxide, are highly beneficial for applications in which electrical conductivity is important, such as in electrodes. However, these materials have some limitations, as they are not very stable chemically at temperatures above 1600 °C, while they can be damaged by thermal cycling at temperatures above 1500 °C and cannot withstand rapid heating. These issues reduce their suitability for applications requiring high-temperature resilience. In this regard, authors in [10] studied the effect of infrared radiation synthesized in the furnace of the NFC photocatalyst ZB-2. This catalyst was added in small amounts (from 0 to 8%) to the popular brand of welding electrode MR-3 to evaluate its welding and technological characteristics. The results indicate that optimal welding and technological properties are achieved with a 2% ZB-2 additive in the electrode coating.

This study builds on previous research by further evaluating the effect of a 2% ZB-2 photocatalyst additive on the coating of MR-3 electrodes and its influence on the quality and mechanical properties of welded AISI 1017 carbon steel joints. The novelty of this work lies in the development and testing of these new welding electrodes, comparing their performance in weld morphology, microstructure, and mechanical properties against widely used ESAB E6013 electrodes.

II. EXPERIMENTAL PROCEDURE

The experiments involved welding a 20 cm line on rectangular AISI 1017 steel plates (200 mm \times 100 mm \times 1.8 mm). Prior to welding, the plates were cleaned with acetone, and then they were joined using SMAW in a butt joint configuration, as shown in Figure 1.

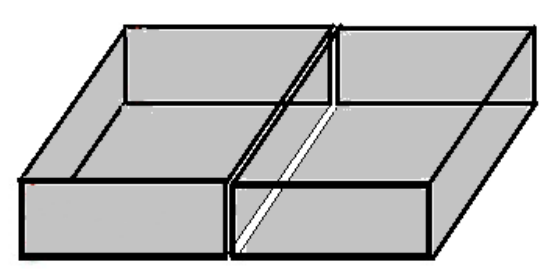


Fig. 1. Butt joint design.

E6013 and IMAN-8 electrodes with a diameter of 2.6 mm and 2.2 mm, respectively, were used as filler material. During

SMAW welding, the current was set at 40 A, while the arc voltage was determined by the arc length, which the welder manually controlled. The chemical composition of low carbon AISI 1017 steel plates, electrodes E6013, and IMAN-8 welding rods [11] is given in Tables I, II, and III, respectively.

TABLE I. CHEMICAL COMPOSITION OF MEDIUM-LOW AISI 1017 STEEL WEIGHT %

Ī	Element	C	Fe	Mn	P	S
ſ	weight %	0.14-0.20	99.11-99.56	0.30-0.60	≤0.04	≤0.05

TABLE II. CHEMICAL COMPOSITION OF ESAB E6013 WELDING ROD (AWS: SFA 5.1 E6013)

I	Element	C	Mn	Si	P	S
	weight %	0.08	0.46	0.22	0.023	0.020

TABLE III. CHEMICAL COMPOSITION OF IMAN-8 WELDING ROD (SV-08A, GOST 2246-70 [11])

Element	C	Cr	Mn	Cu	Ni
weight %	≤0.1	≤0.12	0.35-0.60	≤0.25	≤0.30
Element	Si	P	S		
weight %	≤0.03	≤0.02	≤0.03		

After welding, the samples were extracted while avoiding the starting and ending points of the weld, as displayed in Figure 2. The morphology of the SMAW welds performed using ESAB E6013 and IMAN-8 electrodes was analyzed to assess their structural characteristics. Before the investigation, the samples were polished up to 1200-grit fineness, followed by a cloth polishing to a 0.05 µm alumina surface finish. The AISI 1017 weld zone was etched using nital solution (95 cc ethylene + 5 cc HNO₃). The weld bead features were examined with an optical microscope using Motic software (version 2, Motic Images 3.0, Xiamen, China). Additionally, the microstructural evolution of the fusion zone in both SMAW welds was analyzed using a JEOL JSM-7600F Scanning Electron Microscope (SEM).

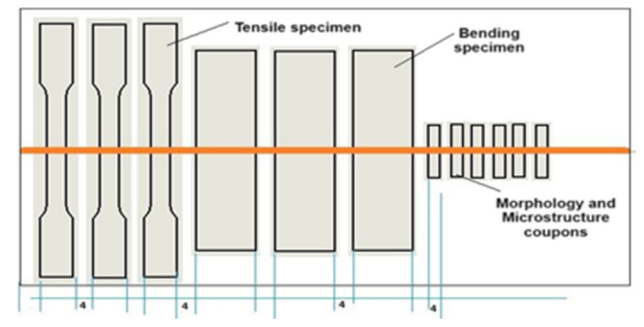


Fig. 2. Test specimen for the tensile test (mm).

Tensile tests were carried out at room temperature (24 $^{\circ}$ C) using a WAW-300E electro-hydraulic servo universal testing machine at a crosshead speed of 0.5 mm/min, a loading rate of 0.5 kN/s, and a strain rate of 1.6 \times 10⁻⁴ s⁻¹. The specimens were cut according to ASTM E8M-04 [12], as depicted in Figure 3. A total of three samples were tested for each weld type to ensure the consistency and reliability of the results. Transverse bend test specimens were prepared according to ASTM E190-14 [13], as portrayed in Figure 4.

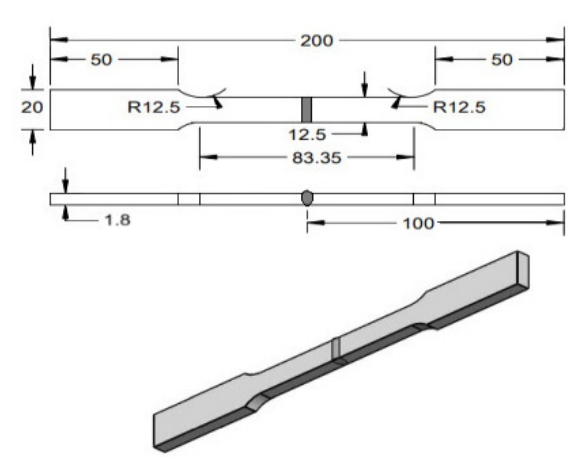


Fig. 3. Tensile test specimen according to ASTM E8M-04 (mm).



Fig. 4. Transverse bend specimen according to ASTM E190-14 (mm).

Vickers hardness tests were performed using an HVS-50 digital hardness tester with a standard load of 10 kgf and a dwell time of 10 seconds, following the ASTM E-384-99 [14] standard. Hardness measurements were taken along a horizontal line, with indentations spaced approximately 0.5 mm apart. The hardness line measurements were positioned 1 mm below the weld surface, as depicted in Figure 5. The hardness distribution was evaluated for both IMAN-8 and E6013 welds to determine variations in mechanical properties across the weld region.

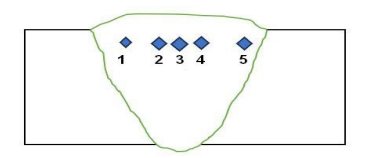


Fig. 5. Vickers hardness horizontal line test specimen according to ASTM E-384-99.

III. RESULTS AND DISCUSSION

The welding technological properties of the ESAB E6013 and IMAN-8 electrodes exhibit several key characteristics. The arc is easily excited and stably maintained, the coating melts evenly without excessive spattering, and the slag ensures the proper formation of the bead seam. Additionally, external inspection revealed no defects, such as cracks or pores in the weld metal, regardless of the electrode used.

Figures 6 and 7 illustrate photographs from both welded joints, captured from the welding side (Figures 6a and 7a) and the back side (Figures 6b and 7b). The visual examination revealed a smooth surface and uniform bead formation on the

front side for both electrodes. However, the weld seam created with the E6013 electrode exhibited a narrower weld width and a lighter surface compared to the IMAN-8 electrode. This indicates a significantly higher wettability of the welded edges with molten electrode metal, and more effective deoxidation of the welded metal when welded with the IMAN-8 electrode. On the back side of the welded plates, the weld seam formed using the IMAN-8 electrode demonstrated a smooth surface and full penetration through the entire thickness of the metal. In contrast, the weld seams on the plates welded with the E6013 electrode exhibited incomplete penetration. The greater penetration capacity of the IMAN-8 welding electrode compared to the ESAB E6013 electrode is evident in the cross-sectional images of the seams presented in Figure 8.

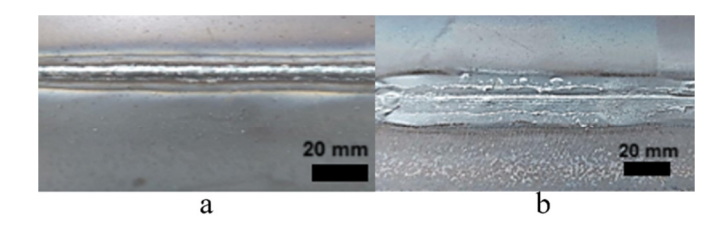


Fig. 6. View of welded join performed with ESAB E6013 electrode from: (a) front side and (b) backside.



Fig. 7. View of welded join performed with IMAN-8 electrode from: (a) front side and (b) backside.

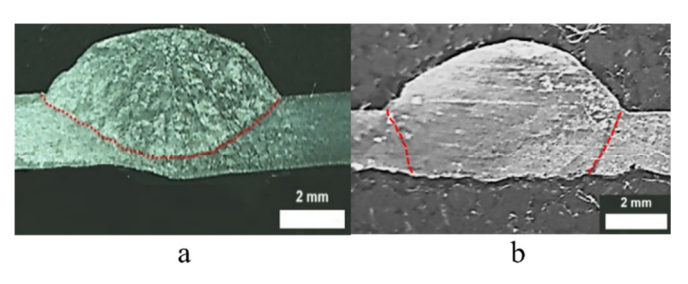


Fig. 8. Macrographs of weld beads performed with: (a) E6013 electrode and (b) IMAN-8 electrode (x4).

The increased rate of melting in the IMAN-8 electrode is likely caused by the addition of a small amount of FNFK ZB-2 additives to its coating. This effect can be explained by the Quantum Tunneling Effect (QTE), a phenomenon where particles or waves overcome a potential barrier due to the accumulation of a significant energy pulse [15]. According to de Broglie, the wavelength of a pulse is determined by the formula $\lambda = h/p$, where λ is the wavelength, h is Planck's constant, and p is the particle momentum. When a large energy pulse, such as photons, is accumulated, the particle wavelength

decreases significantly. These "short-wave" particles can tunnel through a potential barrier, overcoming it even at energies below the barrier height. Unlike the standard tunneling effect, QTE utilizes all photons that interact with functional ceramics and converts them to the desired wavelength. This allows for the efficient use of radiation energy through pulse focusing, exceeding the effective energy of photons over their actual energy [15].

Welds made using the IMAN-8 welding electrode achieved complete penetration in a single pass, unlike those made using the E6013 electrode, which exhibited incomplete penetration. Therefore, to ensure complete penetration in the E6013 welds, a back-side weld bead was carried out, as demonstrated in Figure 9. The mechanical properties of the welded joints were then compared [16].

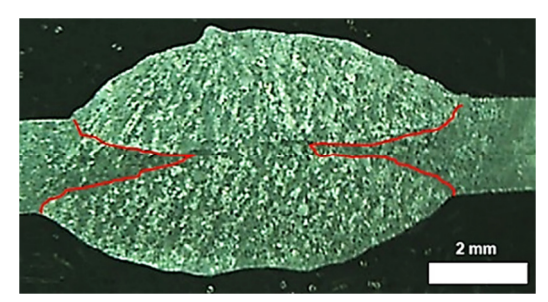


Fig. 9. Macrographs of weld beads performed with E6013 electrode welded on both sides.

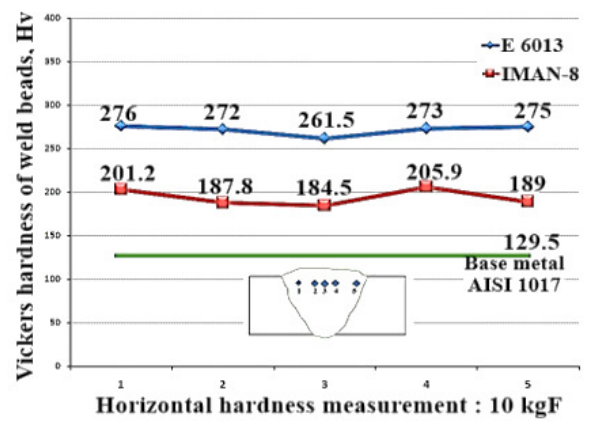


Fig. 10. Results of horizontal hardness (Hv) of welded beads performed with: (a) ESAB E6013 and (b) IMAN-8 electrodes.

The Vickers hardness measurements of the weld metal, conducted horizontally along the welds, revealed higher hardness values for the weld metal produced with E6013 than IMAN-8 electrodes, as shown in Figure 10. At the same time, the hardness at the center of the weld seams was 102% higher than that of the base metal for the E6013 welds and 42% higher for the IMAN-8 welds. At the edges of the weld seams, the hardness increased by 112% and 57%, respectively. Thus, IMAN-8 weld seams have a hardness closer to that of the base metal, which contributes to the greater resistance of the welded joints of carbon steels to dynamic loads compared to welded joints obtained with the E6013 electrodes.

Figures 11 and 12 display images of the specimens after tensile testing. The results show that all welded specimens fractured in the base metal, regardless of the electrode used.



Fig. 11. Tensile specimen for welds performed with E6013 electrode after breaking.



Fig. 12. Tensile specimen for welds performed with IMAN-8 electrode after breaking.

The tensile strength tests revealed that the IMAN-8 electrode welded joints exhibit tensile strength comparable to the base metal, while the E6013 electrode welded joints have a marginally lower tensile strength, as outlined in Table IV.

TABLE IV. TENSILE TEST STRENGTH UTS

Specimen	UTS [MPa] max	UTS [MPa] min	UTS [MPa] average
AISI 1017 both-sided welded with E6013 electrode	397	381	388.66
AISI 1017 welded with IMAN-8 electrode	400	392	394
Medium-low carbon AISI 1017 steel	401	388	393.6

A comparative analysis of the strength coefficient of the welded joints (UTSwj/UTSbm) was carried out, showing the ratio of the strength of the welded joint (UTSwj) to the strength of the base metal (UTSbm). These results exhibit that the E6013 welds had a strength coefficient of 0.987, whereas the IMAN-8 welds achieved 1.001, as presented in Table V. According to the Interstate Standard GOST 34233.1-2017 [17], the minimum strength coefficient required for butt welds with manual root welding is 1.0, while one-sided butt welds must meet a minimum of 0.9. The E6013 welds fell below the required standard, whereas the IMAN-8 welds exceeded it, complying with international standards.

Furthermore, the relative elongation of the IMAN-8 welds is slightly higher than that of the E6013 welds, but lower than that of the base metal, as shown in Table VI. Additionally, bending tests were conducted on the welded joints, and the results indicate high bending angle values for both electrode types, as portrayed in Table VII. Figure 13 depicts the specimens after the bending tests, which demonstrated good results for the welds obtained when welding with both tested electrodes.

TABLE V. STRENGTH COEFFICIENT OF WELDED JOINTS (UTSWJ/UTSBM)

Specimen	UTSwj [MPa]	UTSbm [MPa]	UTSwj/ UTSbm
AISI 1017 both-sided welded with E6013 electrode	388.6	393.6	0.987
AISI 1017 welded with IMAN-8 electrode	394.0	393.6	1.001

TABLE VI. ELONGATION AT BREAK (IN 88 MM)

Specimen	δ [%] max	δ [%] min	δ [%] average
AISI 1017 both-sided welded with E6013 electrode	11.5	13.4	12.6
AISI 1017 welded with IMAN-8 electrode	11.4	13.8	13.0
Medium-low carbon AISI 1017 steel	15.4	16.8	16.2

TABLE VII. BENDING TEST FACE TEST

Specimen	Strength max [MPa]	Bend angle [°]
AISI 1017 both-sided welded with E6013 electrode	1390	180
AISI 1017 welded with IMAN-8 electrode	1375	180



Fig. 13. Welded samples of bending test performed with: (a) ESAB E6013 electrode and (b) IMAN-8 electrode.

The microstructural analysis, as can be seen in Figures 14 and 15, showed that the improved mechanical properties of the IMAN-8 welds were likely due to a finer microstructure and a uniform distribution of pearlite throughout the weld volume. Overall, the IMAN-8 welding electrode offers significant advantages over the widely used E6013 electrode, increasing welding productivity for carbon steel structures by up to two times while reducing welding costs and energy consumption by up to 50%. This ensures the production of high-quality welded joints, making the IMAN-8 electrode a superior alternative in welding applications.

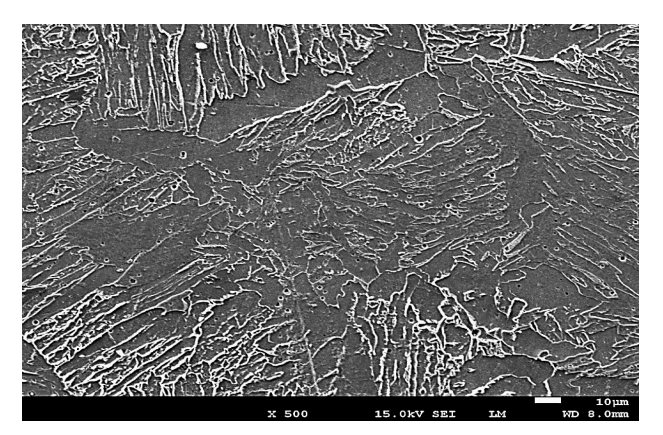


Fig. 14. SEM image for specimen welded by ESAB E6013 electrode (X500).

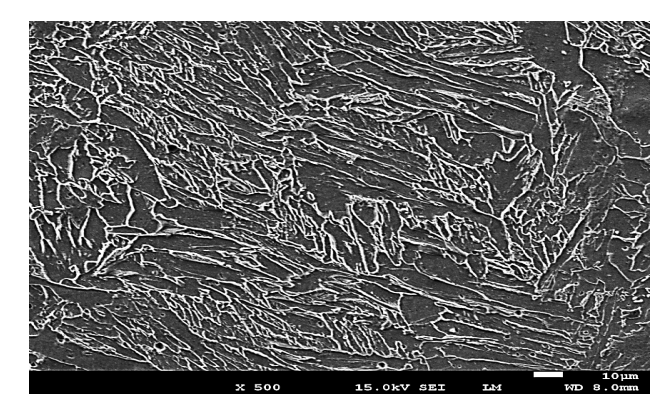


Fig. 15. SEM image for specimen welded by IMAN-8 electrode (X500).

IV. CONCLUSION

The present investigation constitutes a comparative study of the morphology and mechanical properties of welded joints produced using IMAN-8 electrodes, which contain Photocatalysts of Nanostructured Functional Ceramics (PNFC) brand ZB-2 additives, and ESAB E6013 electrodes. The microstructure investigation revealed that the weld metal microstructure produced using IMAN-8 electrodes exhibited a finer grain size and a more uniform distribution of pearlite compared to welds produced with E6013 electrodes. The hardness of the weld metal obtained using IMAN-8 electrodes was higher than that of the base metal but lower than that of welds made using E6013 electrodes. The tensile testing showed that welded joints produced with IMAN-8 electrodes had slightly higher tensile strength and relative elongation than those made with E6013 electrodes. The utilization of IMAN-8 electrodes enhances welding productivity for carbon steel structures and components by up to twofold while reducing welding costs and energy consumption by up to 50%. The former also ensures high-quality welds. Based on these results, IMAN-8 electrodes have the potential for improved performance in welding applications. However, further research is needed to investigate the long-term performance and application of IMAN-8 electrodes in different welding environments.

REFERENCES

- [1] C. Y. A. Nalle, M. B. Aditya, F. G. A. P. Putra, M. N. Nalle, and R. P. Sumarta, "Analysis of Electric Current on Aluminum Plate Welding Using MMA (Manual Metal Arc) Method," *Proceeding of International Conference on Artificial Intelligence, Navigation, Engineering, and Aviation Technology (ICANEAT)*, vol. 1, no. 1, pp. 144–146, Jan. 2024, https://doi.org/10.61306/icaneat.v1i1.222.
- [2] M. I. Qazi, R. Akhtar, "Application of Taguchi Method for Optimization of Tensile Strength of Shielded Metal Arc Welding (SMAW) Process for Steel SA 516 Grade 70," *International Journal of Progressive Sciences and Technologies (IJPSAT)*, vol. 17, no. 2, pp. 97-103, Nov. 2019, https://doi.org/10.52155/IJPSAT.V17.2.1434.
- [3] R. Lostado-Lorza, S. Ruíz-González, C. Sabando-Fraile, and M. Corral-Bobadilla, "Shielded Metal Arc Welding (SMAW): Determining the Thermal Fields With FEM and RSM," in 2024 9th International Conference on Smart and Sustainable Technologies (SpliTech), Bol and Split, Croatia, Jun. 2024, pp. 1–6, https://doi.org/10.23919/SpliTech61897.2024.10612553.
- [4] B. Asati and R. S. Vidyarthy, "A Method for Evaluation of Welding Performance of SMAW Electrodes," in Advances in Industrial Machines and Mechanisms, Y. V. D. Rao, C. Amarnath, S. P. Regalla, A. Javed, and K. K. Singh, Eds. Singapore: Springer Singapore, 2021, pp. 597– 608.
- [5] S. B. Sapozhkov and E. M. Burakova, "The Study of Complex (Ti, Zr, Cs) Nanopowder Influencing the Effective Ionization Potential of Arc Discharge When Mma Welding," *IOP Conference Series: Materials Science and Engineering*, vol. 142, Aug. 2016, Art. no. 012018, https://doi.org/10.1088/1757-899X/142/1/012018.
- [6] M. Kuznetsov and E. Zernin, "Nanotechnologies and nanomaterials in welding production (review)," *Welding International*, vol. 26, no. 4, pp. 311-313, Nov. 2011, https://doi.org/10.1080/09507116.2011.606158.
- [7] S. V. Makarov and S. B. Sapozhkov, "Use of Complex Nanopowder (Al2O3, Si, Ni, Ti, W) in Production of Electrodes for Manual Arc Welding," World Applied Sciences Journal 22, pp. 87–90, 2013.
- [8] S. Mahajan and R. Chhibber, "Design and Development of Shielded Metal Arc Welding (SMAW) Electrode Coatings Using a CaO-CaF2-SiO2 and CaO-SiO2-Al2O3 Flux System," JOM, vol. 71, no. 7, pp. 2435–2444, Jul. 2019, https://doi.org/10.1007/s11837-019-03494-9.
- [9] V. Kumar, R. Chhibber, and S. Mahajan, "Investigations on wetting and structural behavior using CaF₂-SiO₂-CaO-22.5%TiO₂ SMAW electrode coating for AUSC applications," *Proceedings of the Institution of Mechanical Engineers, Part L: Journal of Materials: Design and Applications*, vol. 237, no. 8, pp. 1861–1873, Aug. 2023, https://doi.org/10.1177/14644207231159833.
- [10] R. Saidov, R. Rakhimov, K. Touileb, and S. Abduraimov, "A Study of the Influence of Additives of Nanostructured Functional Ceramics in the Coating of Welding Electrodes on their Welding and Technological Properties," *Engineering, Technology & Applied Science Research*, vol. 14, no. 6, pp. 18711–18717, Dec. 2024, https://doi.org/ 10.48084/etasr.8741.
- [11] GOST 2246-70: Welding steel wire. Specifications. Moscow: State Committee for Standards of the Council of Ministers of the USSR, 1970.
- [12] ASTM E8M-04: Standard Test Methods for Tension Testing of Metallic Materials. West Conshohocken, PA, USA: ASTM International, 2004.
- [13] ASTM E190-14: Standard Test Method for Guided Bend Test for Ductility of Welds. West Conshohocken, PA, USA: ASTM International, 2014.
- [14] ASTM E384-99: Standard Test Method for Microindentation Hardness of Materials. West Conshohocken, PA, USA: ASTM International, 1999.
- [15] R. K. Rakhimov and E. V. Kim, "Radiation emitting ceramic materials and devices containing same," US5350927A, Sep. 27, 1994.
- [16] A.A. Rybakov, S.E. Semenov, T.N Filipchuk, "Properties of weld metal of double-sided welded joints of pipes made of high-strength microalloyed steel," *Automatic welding*, Vol. 5, pp. 40-45, 2013.
- [17] GOST 34233.1-2017: Vessels and apparatuses. Strength calculation standards and methods. Moscow. Euro-Asian Council for Standardization, Metrology and Certification (EASC), 2018.